

# 3-*O*-Methyl-6-<sup>18</sup>F-Fluoro-L-Dopa, a New Tumor Imaging Agent: Investigation of Transport Mechanism In Vitro

Ralf Bergmann, PhD<sup>1</sup>; Jens Pietzsch, PhD<sup>1</sup>; Frank Fuechtner, PhD<sup>1</sup>; Beate Pawelke, PhD<sup>1</sup>; Bettina Beuthien-Baumann, MD<sup>2</sup>; Bernd Johannsen, PhD<sup>1</sup>; and Joerg Kotzerke, MD<sup>2</sup>

<sup>1</sup>Institut fuer Bioorganische und Radiopharmazeutische Chemie, PET Zentrum Rossendorf, Forschungszentrum Rossendorf, Dresden, Germany; and <sup>2</sup>Klinik und Poliklinik fuer Nuklearmedizin, Technische Universitaet Dresden und PET Zentrum Rossendorf, Dresden, Germany

<sup>18</sup>F-Labeled amino acids represent a promising class of imaging agents in tumors, particularly brain tumors. However, the determination of their potential to image peripheral tumors, possibly depending on individual transport characteristics, still remains an area of investigation. The present study investigated the transport mechanism for 3-*O*-methyl-6-<sup>18</sup>F-fluoro-L-dopa (OMFD), a novel <sup>18</sup>F-labeled phenylalanine derivative, into tumor cells. **Methods:** OMFD has routinely and reliably been prepared for clinical use in 20%–25% radiochemical yield (decay corrected, related to <sup>18</sup>F-F<sub>2</sub>) using 6-<sup>18</sup>F-fluoro-L-3,4-dihydroxyphenylalanine preparation devices with minor modifications. In vitro uptake assays with HT-29 (human colon adenocarcinoma) cells, FaDu (squamous cell carcinoma) cells, and RBE4 (immortalized rat brain endothelial) cells were performed with OMFD under physiologic amino acid concentrations without and with the competitive transport inhibitors 2-aminobicyclo-[2,2,1]-heptane-2-carboxylic acid and α-(methylamino)isobutyric acid plus serine and without or with Na<sup>+</sup>. **Results:** Transport inhibition experiments using specific competitive inhibitors demonstrated that uptake of OMFD in all cell lines tested was mediated mainly by the sodium-independent high-capacity amino acid transport systems. The highest OMFD uptake was in FaDu cells. **Conclusion:** OMFD seems to be a promising PET tracer for imaging of amino acid transport in tumors.

**Key Words:** amino acid transport; <sup>18</sup>F; PET; radiotracer

**J Nucl Med 2004; 45:2116–2122**

**R**adiolabeled amino acids are becoming increasingly useful as tracers for the delineation of tumors, particularly brain neoplasms. Over the past 2 decades, a variety of labeled amino acids have been synthesized and evaluated for such a potential in oncology (1,2). In the field of PET, amino acids labeled with <sup>18</sup>F are of particular interest because of its advantageously short half-life—only 20 min—

compared with <sup>11</sup>C. Recently, improved labeling procedures have overcome some limitations of tracer synthesis for routine PET application, and new <sup>18</sup>F-labeled amino acids, such as *O*-(2-<sup>18</sup>F-fluoroethyl)-L-tyrosine (FET), have been introduced (3–6). Our own studies with 3-*O*-methyl-6-<sup>18</sup>F-fluoro-L-dopa (OMFD), known as a metabolite of 6-<sup>18</sup>F-fluoro-L-3,4-dihydroxyphenylalanine, revealed promising tumor-imaging properties for this compound (7,8). The synthesis of OMFD might significantly be improved so that it finds widespread application (9). We hypothesized that OMFD will be transported by the Na<sup>+</sup>-independent transport system L, which is most reactive with both branched chain and aromatic neutral amino acids and is often characterized using the selective nonmetabolizable analog 2-aminobicyclo-[2,2,1]-heptane-2-carboxylic acid (BCH) (3). The present study aimed at the mechanisms involved in specific transport of OMFD into tumor cells. Therefore, human colon adenocarcinoma cell line HT-29 was used as an accepted tumor model. Considering the cellular, tissue, and microenvironmental heterogeneity of tumors, for the present study the human squamous cell carcinoma model cell line FaDu was also studied. Furthermore, additional experiments were performed using immortalized rat capillary cerebral endothelial cell RBE4 as an accepted model of microvascular endothelium.

## MATERIALS AND METHODS

### OMFD Tracer Synthesis

OMFD was synthesized as published previously (9). Briefly, the synthesis of OMFD starts from *N*-formyl-3-*O*-methyl-4-*O*-*boc*-6-trimethylstannyl-L-dopa-ethyl ester and proceeds as shown schematically in Figure 1.

### Cell Culture

**HT-29 Cell Line.** The HT-29 cell line was obtained from the European Collection of Cell Cultures (reference number 91072201). HT-29, which is established from primary colon adenocarcinoma, is described as heterotransplantable and as forming well-differentiated grade I tumors. The cells were routinely cultured in 75-cm<sup>2</sup> flasks with McCoy's 5A medium containing a

Received Mar. 26, 2004; revision accepted Jul. 21, 2004.

For correspondence or reprints contact: Ralf Bergmann, PhD, Forschungszentrum Rossendorf, P.O. Box 51 01 19, D-01314 Dresden, Germany.

E-mail: r.bergmann@fz-rossendorf.de

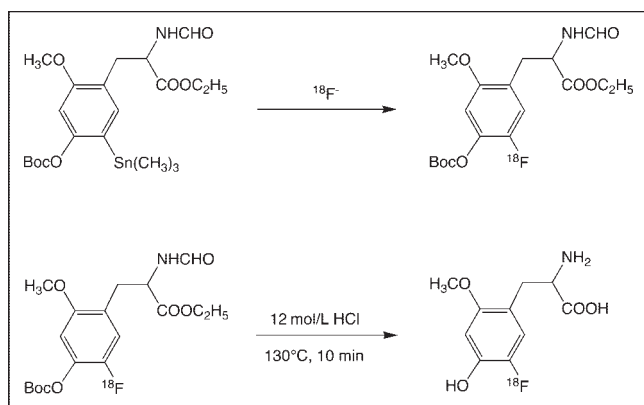


**FIGURE 1.** Reaction scheme of synthesis of OMFD (9).

2 mmol/L concentration of GlutaMAX-I (Gibco BRL), 10% fetal bovine serum (Sigma), and 1% penicillin/streptomycin (10,000 U/10,000  $\mu\text{g}/\text{mL}$ ; Biochrom KG) at 37°C in a humidified atmosphere of 5%  $\text{CO}_2$ . The medium was routinely renewed 3 times weekly. Two days before the *in vitro* experiments, the cells were trypsinized and plated on 24-well ( $5 \times 10^4$  cells per well) flat-bottom tissue culture plates (Cell+; Sarstedt, Inc.).

**FaDu Cell Line.** FaDu cells established from human hypopharyngeal squamous cell carcinoma were cultivated in Dulbecco's minimal essential medium (MEM) with a 2 mmol/L concentration of GlutaMAX-I (Biochrom KG) completed with 10% fetal bovine serum (Biochrom KG), 1 mmol of sodium pyruvate per liter, 1% MEM nonessential amino acids (Biochrom KG), 20 mmol of *N*-(2-hydroxyethyl)piperazine-*N'*-(2-ethanesulfonic acid) (HEPES) buffer (Biochrom KG) per liter, and 1% penicillin/streptomycin (10,000 U/10,000  $\mu\text{g}/\text{mL}$ ) (10). At confluence the cells were washed with phosphate-buffered saline (PBS) and harvested with 0.025% trypsin/ethylenediaminetetraacetic acid (Biochrom KG). Cells were counted, centrifuged, and diluted in PBS as  $10^8$  cells per milliliter. These cells were cultivated at 37°C and 5%  $\text{CO}_2$  in RPMI 1640 medium with a 2 mmol/L concentration of GlutaMAX-I (Life Technologies GmbH) completed with 10% stripped fetal bovine serum (Greiner), 1 mmol of sodium pyruvate per liter, 1% MEM nonessential amino acids, 20 mmol of HEPES buffer per liter, 1% penicillin/streptomycin (10,000 U/10,000  $\mu\text{g}/\text{mL}$ ), and 10  $\mu\text{g}$  of insulin per milliliter. The solution used for transport experiments was a modified culture medium consisting of  $\alpha$ -MEM/Ham's F10 (Gibco) (1:1 v/v) supplemented with 2 mmol of glutamine per liter and 1% (v/v) albumin. Cells were plated on 24-well ( $5 \times 10^4$  cells per well) flat-bottom tissue culture plates (Cell+).

**RBE4 Cell Line.** Immortalized rat capillary cerebral endothelial cells (RBE4) were kindly supplied by Dr. Françoise Roux (Institut National de la Santé et de la Recherche Médicale, Unité 26, Hôpital Fernad Widal) (11–13). RBE-4 cells were grown in culture medium consisting of  $\alpha$ -MEM/Ham's F10 (1:1 v/v) supplemented with 2 mmol of glutamine per liter, 10% heat-inactivated fetal calf serum (Sigma), 1 ng of basic fibroblast growth factor (Boehringer Mannheim) per milliliter, and 300  $\mu\text{g}$  of geneticin (G418; Sigma) per milliliter in humidified 5%  $\text{CO}_2/95\%$  air at 37°C. For tracer experiments performed with RBE4 cells, cells of passage 20–40 were seeded into 24-well flat-bottom tissue culture plates (Cell+) at day 3 or 4 after plating. The cell densities at that time were  $5 \times 10^5$  cells per well ( $87 \pm 35$   $\mu\text{g}$  of protein per well). Washing

solution for clearing of the extracellular space was phosphate-buffered solution containing  $\text{Mg}^{2+}$  (0.5 mmol/L) and  $\text{Ca}^{2+}$  (0.9 mmol/L) ( $\text{PBS}^{2+}$ ).

## Uptake Experiments

The experiments were performed in RPMI 1640 medium with modified amino acid concentrations corresponding to human plasma amino acid levels including tyrosine. Before the incubation with OMFD, the cells were preincubated for 10 min at 37°C in 250  $\mu\text{L}$  of medium or incubation buffer with and without  $\text{Na}^+$ . In the case of  $\text{Na}^+$ -free buffer, the  $\text{Na}^+$  was replaced by choline. After preincubation of the cells, 250  $\mu\text{L}$  of incubation medium with OMFD (2 MBq/mL) were added, and the samples were incubated at 4°C or 37°C for 1, 2, 3, 5, 7, and 10 min. After tracer uptake had been stopped with 1 mL of ice-cold PBS, the cells were washed 3 times with PBS at 4°C and dissolved in 0.5 mL of a 0.1 mol/L concentration of NaOH plus 1% sodium dodecylsulfate. The radioactivity in the cells was measured with a well counter (COBRA II; Packard). The protein concentration in the samples was determined by the Lowry method (Sigma). The energy dependence of tracer uptake was characterized by comparing the uptake kinetics of OMFD at both 37°C and 4°C or in experiments using various concentrations of  $\text{NaN}_3$  (ranging from 0 to 15 mmol/L). To study the relationship between OMFD and  $^3\text{H}$ -L-leucine uptake in HT-29 cells containing various concentrations of BCH (ranging from 0 to 15 mmol/L), the cells were preincubated in RPMI 1640 medium with modified amino acid concentrations as described above. Then, the medium was replaced by the same medium containing 1 MBq of OMFD and 0.1 MBq of  $^3\text{H}$ -L-leucine per milliliter, and the cells were incubated in 0.25 mL for 5 min. Uptake was terminated by 3 rapid washes with ice-cold  $\text{PBS}^{2+}$ , and the cells were lysed in 0.5 mL of 0.1N NaOH containing 0.1% sodium dodecylsulfate. Aliquots (100  $\mu\text{L}$ ) were used to count the total  $^{18}\text{F}$  activity in a well  $\gamma$ -counter (COBRA II), and the tritium activity was counted in 4 mL of scintillate (UltimaGold; Perkin-Elmer) 2 d later.

## Competitive Inhibition Experiments

To characterize the transport system, inhibition experiments were performed with the specific competitive inhibitors BCH for system L,  $\alpha$ -(methylamino)isobutyric acid (MeAIB) for system A, and serine for system ASC. The concentration of the inhibitors used was 10 mmol/L or varied between 0 and 15 mmol/L. Experiments were performed with increasing concentrations of OMFD to investigate the capacity of the transport system. After preincubation of the cells in 250  $\mu\text{L}$  of this medium for 10 min at 37°C, 250  $\mu\text{L}$  of incubation medium with OMFD (2 MBq/mL) with one or more of the inhibitors were added, and the samples were incubated at 37°C for 2 min or for 1, 2, 3, 5, 7, and 10 min. After the tracer uptake had been stopped with 1 mL of ice-cold PBS, the cells were washed 3 times and were dissolved, and the radioactivity and protein concentrations were measured as described above. To determine the median effective concentration ( $\text{EC}_{50}$ ) of BCH inhibition of the tracer transport in HT-29 cells, kinetic curves of the activity at time  $t$  ( $A_t$ ) were fitted using an equation for the monoexponential association ( $A_t = A_0 \times [1 - \exp(-k \times t)] + \text{NSB}$ ). The curve starts at nonspecifically bound activity (NSB) and increases to a plateau at  $A_0 + \text{NSB}$  ( $A_0$  equals maximal activity) with a rate constant  $k$ . Then, the initial rate constants ( $k$ ) were plotted against the log of BCH concentration, in mmol/L. This curve was fitted for a sigmoid dose-response curve using  $Y = \text{bottom} + (\text{top} - \text{bottom}) / (1 + 10^{[\log(\text{EC}_{50}) - X]})$ , where  $X$  is the logarithm of concentration,  $Y$  is the rate at a defined BCH con-

centration using  $BCH_i$  and  $k_i$  obtained from the experiments before, and  $Y$  starts at bottom and goes to top with a sigmoid shape. The kinetic data were processed using Prism (version 3.00; Graph-Pad, Inc.).

### Release Experiments

After the cells had been preloaded with tracer through 60 min of incubation with OMFD, the medium was replaced by 1 mL of tracer-free culture medium without (control) or with 2 mmol of BCH per liter, and the samples were incubated at 37°C for 1, 2, 3, 5, 7.5, and 10 min. After the incubation, the medium was removed and the cells were washed 4 times with ice-cold PBS. Dissolving and measuring of the activity in the cell pellets were performed as described above.

### Acid Precipitation

The cells were incubated with OMFD for 30 min as described above, and the medium was then removed and the cells were detached with 1 mL of trichloroacetic acid (1%). After 10 min on ice, the samples were centrifuged at 20,000g for 3 min. The supernatant was removed and the pellet was washed 3 times in trichloroacetic acid (1%). Dissolving and measuring of the activity in the acid-precipitable fraction were done as described above. The collected supernatant underwent high-performance liquid chromatography as previously described (14).

## RESULTS

OMFD cellular uptake studies were conducted on established tumor-model cell lines HT-29 and FaDu, and OMFD cellular uptake studies were performed on immortalized rat capillary cerebral endothelial cells RBE4. The latter are an accepted model of microvascular endothelium and probably the most extensively characterized cell culture model for mechanistic studies of the blood-brain barrier. The tracer amino acid OMFD was taken up quickly by all cells studied. As a representative example, Figure 2A shows the kinetics of OMFD uptake in HT-29 cells without and with the specific L-amino acid transport system inhibitor BCH. With increasing concentrations of BCH in HT-29 cells, the

OMFD uptake velocity and magnitude were significantly decreased (Fig. 2B). FaDu and RBE4 cells showed similar results. The  $EC_{50}$  of BCH inhibition was calculated from the sigmoid dose-response curve by a nonlinear curve fit of the initial uptake velocity as  $2.2 \pm 0.1$  mmol/L for HT-29 cells,  $0.2 \pm 0.1$  mmol/L for FaDu cells, and  $0.7 \pm 0.2$  mmol/L for RBE4 cells.

To further characterize the specific cellular uptake of OMFD, competitive inhibition experiments were performed. Therefore, in addition to BCH, the specific amino acid transport inhibitors MeAib and serine were used to inhibit all major transport systems of neutral amino acids (Fig. 3). In the presence of BCH, the OMFD uptake was decreased by approximately 80% in all cell lines studied when compared with controls. MeAib and serine alone or in combination did not affect cellular uptake of OMFD. To determine the presence of  $Na^+$ -independent amino acid transport processes in all cell lines, cellular uptake experiments were performed in the presence and absence of  $Na^+$ . Substitution of sodium ions by choline did not influence uptake of OMFD in HT-29 cells, FaDu cells, or RBE4 cells (Fig. 3). As a result, cellular uptake of OMFD was recognized to be sodium independent.

To further characterize specific properties of cellular OMFD transport, the release of OMFD in the presence and absence of BCH was studied in HT-29 cells after preloading of OMFD (Fig. 4). In addition, because the L-type amino acid transport system is an exchanging transporter, measurement of the extent of OMFD release after preincubation with OMFD was exemplary in HT-29 cells. The release rate of  $^{18}F$ -activity from HT-29 cells was as fast as uptake. The estimated values were  $0.47 \pm 0.06$  for rate constant uptake  $k_1$  control,  $0.20 \pm 0.02$  for rate constant uptake  $k_1$  BCH 6 mmol/L,  $0.53 \pm 0.03$  for rate constant efflux  $k_2$  control, and  $0.57 \pm 0.04$  for rate constant efflux  $k_2$  BCH 6 mmol/L. Efflux of the OMFD did not significantly differ between the

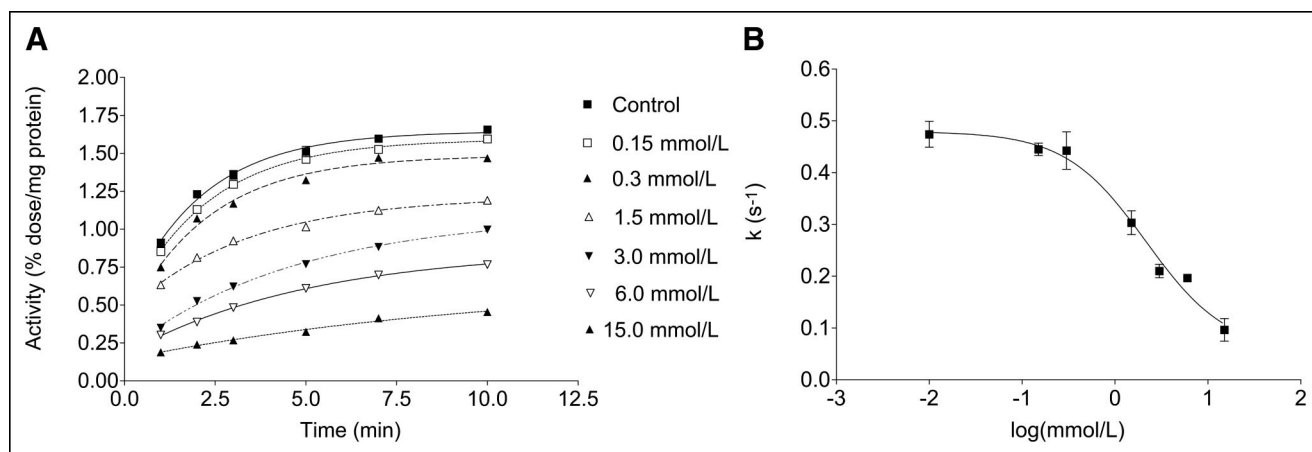


**FIGURE 2.** Representative curves showing time course of OMFD uptake in HT-29 cells without (control) and with various concentrations of BCH in incubation medium (A) and OMFD uptake velocity ( $k$ ) in HT-29 cells in presence of various concentrations of BCH (B). Data are mean  $\pm$  SEM ( $n = 4$ ).

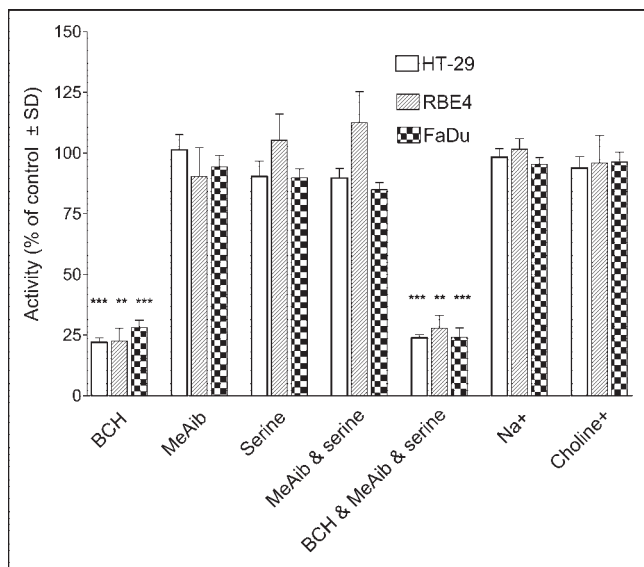


**FIGURE 3.** Influence of specific amino acid transporter inhibitors, sodium, and choline (without sodium) on OMFD uptake in HT-29, FaDu, and RBE4 cells. Data are mean  $\pm$  SEM ( $n = 4$ ). \*\* $P < 0.01$ ; \*\*\* $P < 0.001$  (Student  $t$  test, SPSS software package).

control experiment and the experiment performed in the presence of 6 mmol of extracellular BCH per liter.

To compare functional expression of the L-amino acid transport systems in the 2 tumor cell models, the kinetics of OMFD uptake were compared between HT-29 and FaDu cells as shown in Figures 5A and 5B. Therefore, uptake of OMFD was also measured in the presence of unlabeled OMFD ( $^{19}\text{F}$ -OMFD). Uptake of OMFD was approximately 6-fold higher into FaDu cells than into HT-29 cells. Uptake of OMFD into both HT-29 and FaDu cells was saturable and apparently followed Michaelis–Menten kinetics, with  $K_M = 46.7 \pm 4.44 \mu\text{mol/L}$  and  $V_{\text{max}} = 1.62 \pm 0.06 \text{ nmol/min/mg}$  of protein in HT-29 cells and  $K_M = 99.8 \pm 14.5 \mu\text{mol/L}$  and  $V_{\text{max}} = 14.6 \pm 1.15 \text{ nmol/min/mg}$  of protein in FaDu cells. Data represent the mean  $\pm$  SEM of 3 separate experiments. All uptake experiments were performed with medium; therefore, extracellular and intracellular amino acid concentrations are expected to be near their physiologic concentration.

In further experiments, the relationship between  $^3\text{H}$ -L-leucine uptake and OMFD uptake in HT-29 cells without and with BCH was measured (Fig. 6), and uptake of the 2 compounds was found to correlate closely ( $R^2 > 0.95$ ). At 15 mmol of BCH per liter, uptake of  $^3\text{H}$ -L-leucine was faster than uptake of OMFD. Furthermore, to study the energy dependence of the observed OMFD transport process in HT-29 cells, the OMFD uptake at  $37^\circ\text{C}$  was compared with that at  $4^\circ\text{C}$ . No significant differences were found (Fig. 7A). In a set of experiments in both HT-29 and FaDu cells, oxidative phosphorylation was inhibited by adding increasing concentrations of sodium azide ( $\text{NaN}_3$ , 0–15 mmol/L), which mimics the effects of hypoxia under normoxic con-

ditions (Fig. 7B). However,  $\text{NaN}_3$  did not influence the uptake kinetics. After a 1-h incubation of OMFD with all cell lines studied, only one high-performance liquid chromatography peak of  $^{18}\text{F}$ -activity in the cell lysate could be observed, thus confirming the metabolic stability of the tracer amino acid OMFD found by other studies (7,8). Furthermore, no incorporation of  $^{18}\text{F}$ -activity into proteins could be observed.

## DISCUSSION

In the past, OMFD has been dealt with mainly as a metabolite of 6- $^{18}\text{F}$ -fluoro-L-3,4-dihydroxyphenylalanine that is able to pass the blood–brain barrier, contributes to  $^{18}\text{F}$  uptake in the striatum, and has to be considered for the formulation of a quantitative 6- $^{18}\text{F}$ -fluoro-L-3,4-dihydroxyphenylalanine kinetic model (15). Because OMFD is a methoxy derivative of the amino acid tracer 2- $^{18}\text{F}$ -fluoro-L-tyrosine (3) and could possibly still act as a substrate of the transport system for the large neutral amino acids, it may also have potential as an amino acid transport–based tumor imaging agent.

The possible pathways for the transport of neutral amino acids are described as 3 major systems: A, ASC, and L (16). Systems A and ASC serve mainly for the uptake of amino acids with short, polar, or linear side chains. In contrast, branched and aromatic amino acids enter the cells mainly by system L (17). Therefore, we studied the transport system for OMFD in an adenocarcinoma cell line from colon (HT-29), a head and neck squamous cancer cell line (FaDu), and, as a model of the vascular endothelium, a benign endothelial cell line (RBE4). Only a very few in vitro studies have investigated fluorine-labeled amino acids using tumor cell lines of colorectal cancer or glioma (6,18–20). However,  $^{11}\text{C}$ -methionine was used in vitro on squamous cell carcinoma (21) and was applied clinically to squamous cell head and neck cancer (22). As concluded from studies on 3- $^{123}\text{I}$ -iodo- $\alpha$ -methyl-L-tyrosine (IMT) transport and 4F2 antigen expression in human glioma cells, the phenomenon of in-

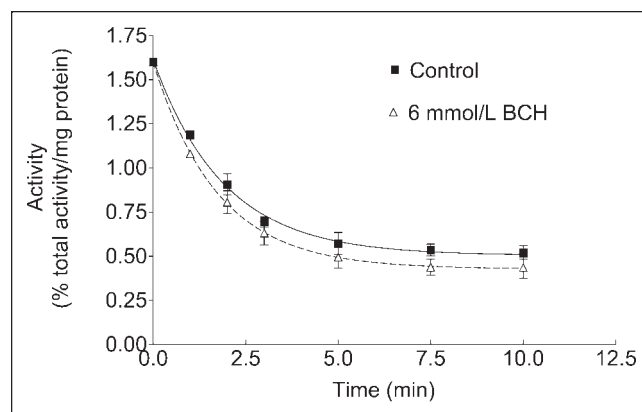


**FIGURE 4.** Kinetics of OMFD release in HT-29 cells in presence and absence of BCH at  $37^\circ\text{C}$  after preloading of OMFD. Data are mean  $\pm$  SEM ( $n = 4$ ).

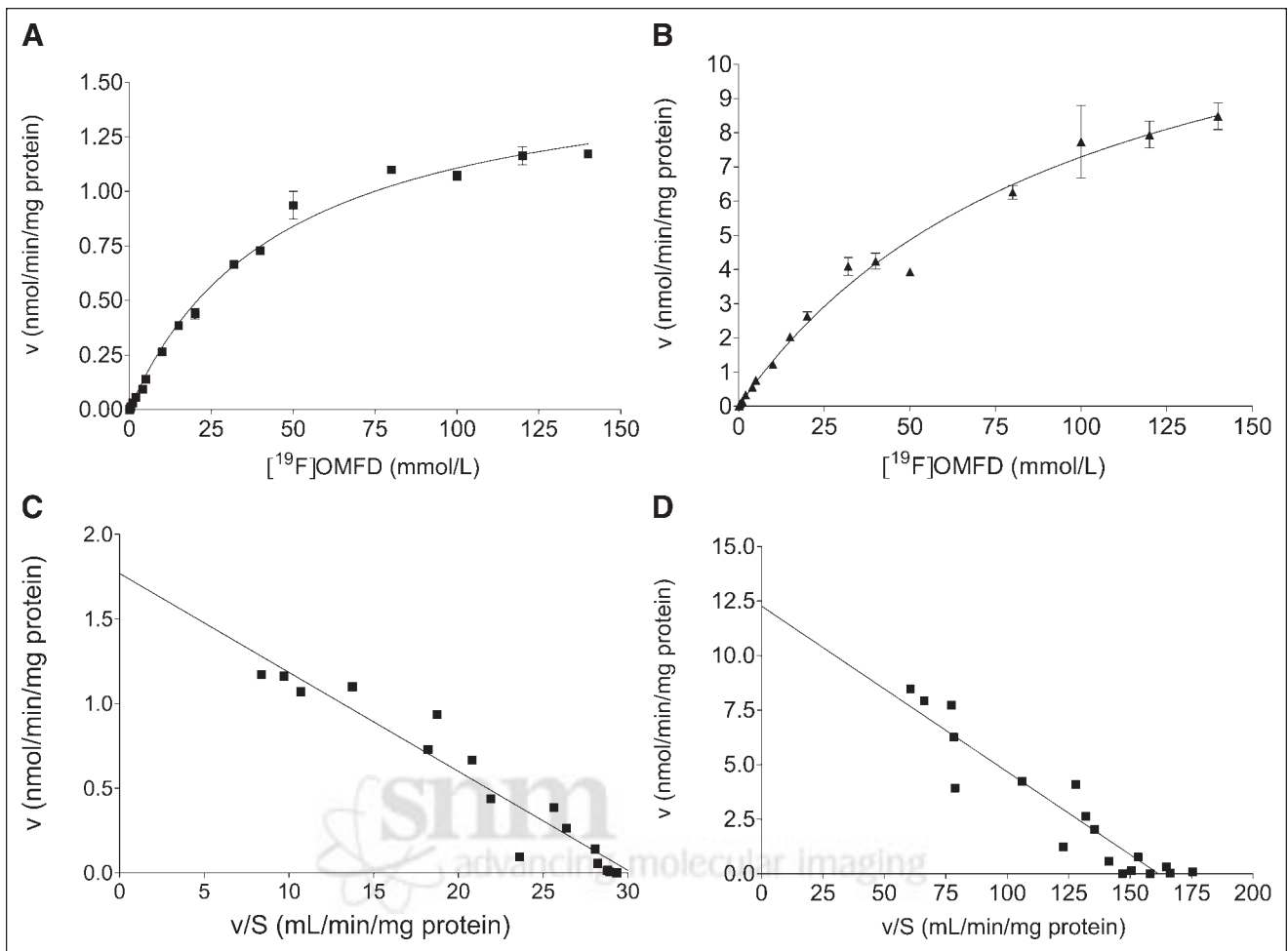


**FIGURE 5.** Concentration-dependent OMFD uptake in adenocarcinoma cells (HT-29) (A) and squamous carcinoma cells (FaDu) (B). OMFD uptake was measured with varying concentrations of unlabeled <sup>19</sup>F-OMFD between 0 and 150  $\mu$ mol/L. Data are mean  $\pm$  SEM ( $n = 4$ ). (C and D) Corresponding Eadie-Hofstee plots.  $v$  = initial velocity of OMFD uptake;  $S$  = substrate concentration.

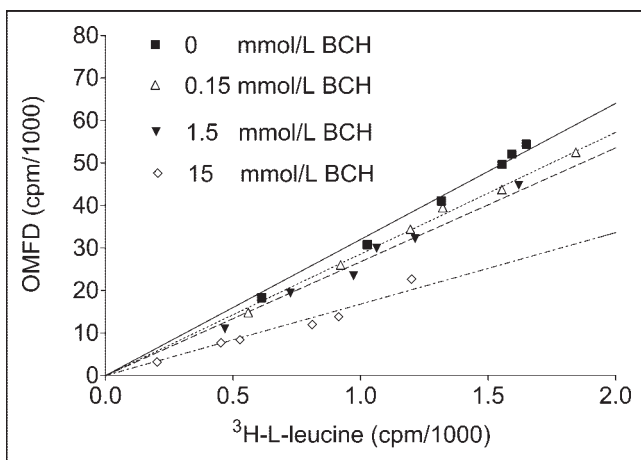


**FIGURE 6.** Comparison of OMFD and <sup>3</sup>H-L-leucine uptake in adenocarcinoma cells (HT-29) in absence and presence of various BCH concentrations after incubation at 1, 2, 3, 5, 7, and 10 min. Data are mean  $\pm$  SEM ( $n = 4$ ).

creased amino acid transport in proliferating cells involves all phases of the cell cycle (23). Therefore, we studied the cells under confluent conditions and synchronization was not necessary. Amino acid transport proteins with overlapping substrate specificities mediate uptake of amino acids in normal and tumor cells. In most cell types, the sodium-independent transporter system L is present and has a broad substrate specificity (24). Expression of amino acid transport proteins differs among several cell types (25). Of note, for the 2 tumor models studied we also found clear differences in cellular OMFD uptake.  $V_{max}$  was higher in FaDu cells by a factor of 6 than in HT-29 cells. On the other hand, the affinity of OMFD to the transport system ( $K_m$ ) was 2 times higher in HT-29 cells than in FaDu cells. These cells strongly differ in their extent of transformation and degree of differentiation, respectively. It is likely that besides influencing physiologic functions, these differences also influence amino transport processes, thus in part explaining the different tracer uptake velocities in HT-29 and FaDu

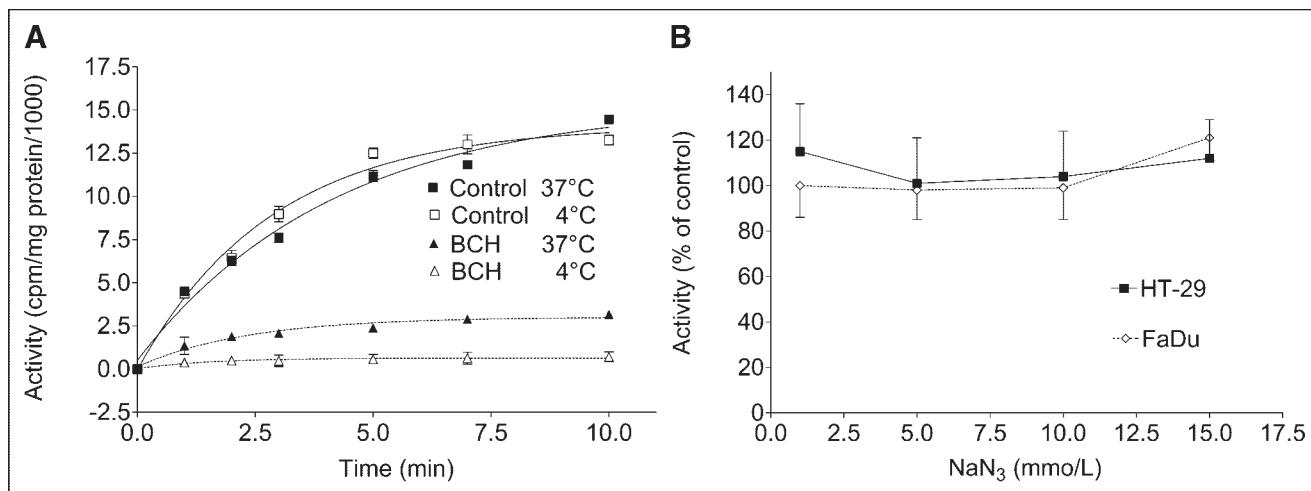


**FIGURE 7.** (A) Influence of incubation temperature on OMFD uptake in adenocarcinoma (HT-29) without (control) and with 6 mmol BCH per liter. (B) Influence of various concentrations of sodium azide on OMFD uptake in adenocarcinoma (HT-29) and squamous carcinoma (FaDu) cells. Data are mean  $\pm$  SEM ( $n = 4$ ).

cells. These differences in kinetic parameters *in vitro* consequently should be considered to influence the absolute accumulation and kinetics of OMFD *in vivo*. Therefore, for clinical applications of OMFD (e.g., to estimate the optimal time frame for PET), kinetic data for various tumor entities will be needed.

Our cellular uptake studies demonstrated, for what is to our knowledge the first time, that OMFD was transported into the cells following apparent first-order kinetics and was saturable by the transported substrate. The transporter affinity of OMFD, described by the half-saturation constant  $K_m$ , is similar to the affinity of other large neutral amino acids to the L-type transporter. The fast release of  $^{18}\text{F}$ -radioactivity from the cells demonstrates that the transport system works as expected in both directions at the cell membrane. The specific inhibition of radioactivity uptake by BCH, which is a specific inhibitor of the L system without inhibition by MeAib and serine, demonstrates that most radioactivity is transported by the L system and that only minor amounts can be transported by other pathways. This finding is supported by the linear correlation between OMFD and leucine uptake in cells. In the present study, we observed saturation of the transport system by nonradioactive  $^{19}\text{F}$ -OMFD. This adds to a controversial discussion as reviewed by Jager (26). In this context, our data seem, in part, to contradict findings showing an increase in L-type amino acid transporter activity when cells were loaded with amino acids. Heiss et al. demonstrated, in colon carcinoma cell line SW 707, that FET is mediated mainly by system L and is sodium independent (18). Furthermore, Heiss et al. could not reach saturation of the L-type amino acid transport system in a colon carcinoma cell line *in vitro* using FET up to a concentration 5 times higher than the normal tyrosine concentration in human plasma. More recently, Lahoutte et al. showed that prior amino acid administration increases IMT tumor accumulation and image contrast *in*

*vivo* (27). This effect possibly can be explained by the increased antiport activity of the L-type amino acid transport system under preloaded conditions. On the other hand, Amano et al. found decreased *in vivo* uptake of L-3-( $^{18}\text{F}$ -fluoromethyl)-L-tyrosine, a fluorinated variant of IMT, when large neutral amino acids were administered beforehand (28). However, for a direct comparison of the *in vitro* results of the present study and both the *in vitro* and the *in vivo* results published by others, the experimental conditions have to be considered, particularly the different cell types and cell culture conditions used and the kind and level of amino acids used for preloading. For example, different extents of transformation and degrees of differentiation for different tumor cells is suspected to influence regulation of amino acid transport systems *in vitro*. In this context, Langen et al. demonstrated that FET uptake in F98 rat glioma cells is sodium dependent (20). Finally, the points raised above imply that, for clinical application of OMFD, the plasma levels of neutral amino acids can influence the uptake kinetics of OMFD (1,2). Corresponding to the sodium independence of the OMFD transport, no energy dependence could be found. Neither reduction of temperature nor inhibition of oxidative phosphorylation by  $\text{NaN}_3$  influenced OMFD accumulation in the colon carcinoma cell line. One would suppose that for clinical tumor imaging, tumor hypoxia, in contrast to microenvironmental factors such as perfusion, will not influence OMFD uptake at the cellular level. Unlike 2- $^{18}\text{F}$ -fluoro-L-tyrosine, described as a tracer for protein synthesis (3), the methoxy derivative OMFD is not incorporated into proteins. From kinetic modeling of 2- $^{18}\text{F}$ -fluoro-L-tyrosine uptake, the transport rate constant of the tracer from plasma to tissue is known to significantly increase in tumors and thus separate normal from pathologic tissue (1). Given this importance of an increased transport rate constant, it is understandable that comparison of amino acids with and without protein incorporation (e.g., FET vs.

L-methyl-<sup>11</sup>C-methionine) revealed almost identical imaging contrast in clinical studies—for example, in patients with brain tumors (29).

## CONCLUSION

Amino acid transport is generally increased in malignant transformation. OMFD demonstrated a saturable and sodium- and energy-independent accumulation in vitro in different tumor cell lines, suggesting its uptake to be mediated exclusively by the sodium-independent large neutral amino acid transport system (L system). This could be confirmed by additional experiments on vascular endothelium cells recognized as being L-amino acid transport system bearing, as published elsewhere. OMFD was not included in the synthesized proteins during the experiments, and no metabolism was detectable in the cells studied. OMFD has the properties of a promising PET tracer for tumor imaging of the functional expression of amino acid transport systems.

## REFERENCES

- Jager PL, Vaalburg W, Pruim J, de Vries EG, Langen KJ, Piers DA. Radiolabeled amino acids: basic aspects and clinical applications in oncology. *J Nucl Med.* 2001;42:432–445.
- Laverman P, Boerman OC, Corstens FH, Oyen WJ. Fluorinated amino acids for tumour imaging with positron emission tomography. *Eur J Nucl Med Mol Imaging.* 2002;29:681–690.
- Coenen HH, Kling P, Stocklin G. Cerebral metabolism of L-[2-<sup>18</sup>F]fluorotyrosine, a new PET tracer of protein synthesis. *J Nucl Med.* 1989;30:1367–1372.
- Kubota K, Ishiwata K, Kubota R, et al. Feasibility of fluorine-18-fluorophenyl-alanine for tumor imaging compared with carbon-11-L-methionine. *J Nucl Med.* 1996;37:320–325.
- Wester HJ, Herz M, Weber W, et al. Synthesis and radiopharmacology of O-(2-[<sup>18</sup>F]fluoroethyl)-L-tyrosine for tumor imaging. *J Nucl Med.* 1999;40:205–212.
- Inoue T, Shibasaki T, Oriuchi N, et al. <sup>18</sup>F alpha-methyl tyrosine PET studies in patients with brain tumors. *J Nucl Med.* 1999;40:399–405.
- Füchtner F, Steinbach J, Vorwieger G. 3-O-methyl-6-[<sup>18</sup>F]fluoro-L-DOPA: a promising substance for tumour imaging. *J Labelled Compds Radiopharm.* 1999; 42(suppl 1):S267–S269.
- Beuthien-Baumann B, Bredow J, Burchert W, et al. 3-O-methyl-6-[(18)F]fluoro-L-DOPA and its evaluation in brain tumour imaging. *Eur J Nucl Med Mol Imaging.* 2003;30:1004–1008.
- Füchtner F, Steinbach J. Efficient synthesis of the <sup>18</sup>F-labelled 3-O-methyl-6-[<sup>18</sup>F]fluoro-L-DOPA. *Appl Radiat Isot.* 2003;58:575–578.
- Rangan SR. A new human cell line (FaDu) from a hypopharyngeal carcinoma. *Cancer.* 1972;29:117–121.
- Roux F, Durieu-Trautmann O, Chaverot N, et al. Regulation of gamma-glutamyl transpeptidase and alkaline phosphatase activities in immortalized rat brain microvessel endothelial cells. *J Cell Physiol.* 1994;159:101–113.
- Regina A, Koman A, Piciotti M, et al. Mrp1 multidrug resistance-associated protein and P-glycoprotein expression in rat brain microvessel endothelial cells. *J Neurochem.* 1998;71:705–715.
- Bergmann R, Brust P, Scheunemann M, et al. Assessment of the in vitro and in vivo properties of a (99m)Tc-labeled inhibitor of the multidrug resistant gene product P-glycoprotein. *Nucl Med Biol.* 2000;27:135–141.
- Vorwieger G, Brust P, Bergmann R, et al. HPLC analysis of the metabolism of 6-[<sup>18</sup>F]fluoro-L-DOPA in the brain of neonatal pigs. In: Carson RE, Daube-Witherspoon ME, Herscovitch P, eds. *Quantitative Functional Brain Mapping with Positron Emission Tomography.* New York, NY: Academic Press, 1998: 285–292.
- Brust P, Bauer R, Walter B, et al. Simultaneous measurement of [<sup>18</sup>F]FDOPA metabolism and cerebral blood flow in newborn piglets. *Int J Dev Neurosci.* 1998;16:353–364.
- Palacin M, Estevez R, Bertran J, Zorzano A. Molecular biology of mammalian plasma membrane amino acid transporters. *Physiol Rev.* 1998;78:969–1054.
- Saier MH Jr, Daniels GA, Boerner P, Lin J. Neutral amino acid transport systems in animal cells: potential targets of oncogene action and regulators of cellular growth. *J Membr Biol.* 1988;104:1–20.
- Heiss P, Mayer S, Herz M, Wester HJ, Schwaiger M, Senekowitsch-Schmidtke R. Investigation of transport mechanism and uptake kinetics of O-(2-[<sup>18</sup>F]fluoroethyl)-L-tyrosine in vitro and in vivo. *J Nucl Med.* 1999;40:1367–1373.
- Martarello L, McConathy J, Camp VM, et al. Synthesis of syn- and anti-1-amino-3-[<sup>18</sup>F]fluoromethyl-cyclobutane-1-carboxylic acid (FMACBC), potential PET ligands for tumor detection. *J Med Chem.* 2002;45:2250–2259.
- Langen KJ, Jarosch M, Muhlensiepen H, et al. Comparison of fluorotyrosines and methionine uptake in F98 rat gliomas. *Nucl Med Biol.* 2003;30:501–508.
- Minn H, Clavo AC, Grenman R, Wahl RL. In vitro comparison of cell proliferation kinetics and uptake of tritiated fluorodeoxyglucose and L-methionine in squamous-cell carcinoma of the head and neck. *J Nucl Med.* 1995;36:252–258.
- Lindholm P, Leskinen S, Lapela M. Carbon-11-methionine uptake in squamous cell head and neck cancer. *J Nucl Med.* 1998;39:1393–1397.
- Langen KJ, Bonnie R, Muhlensiepen H, et al. 3-[<sup>123</sup>I]iodo-alpha-methyl-L-tyrosine transport and 4F2 antigen expression in human glioma cells. *Nucl Med Biol.* 2001;28:5–11.
- Lahoutte T, Caveliers V, Dierickx L, et al. In vitro characterization of the influx of 3-[<sup>125</sup>I]iodo-L-alpha-methyltyrosine and 2-[<sup>125</sup>I]iodo-L-tyrosine into U266 human myeloma cells: evidence for system T transport. *Nucl Med Biol.* 2001;28: 129–134.
- Christensen HN. Distinguishing amino acid transport systems of a given cell or tissue. *Methods Enzymol.* 1989;173:576–616.
- Jager PL. Improving amino acid imaging: hungry or stuffed? *J Nucl Med.* 2002;43:1207–1209.
- Lahoutte T, Caveliers V, Franken PR, Bossuyt A, Mertens J, Everaert H. Increased tumor uptake of 3-(123)I-iodo-L-alpha-methyltyrosine after preloading with amino acids: an in vivo animal imaging study. *J Nucl Med.* 2002;43:1201–1206.
- Amano S, Inoue T, Tomiyoshi K, Ando T, Endo K. In vivo comparison of PET and SPECT radiopharmaceuticals in detecting breast cancer. *J Nucl Med.* 1998; 39:1424–1427.
- Weber WA, Wester HJ, Grosu AL, et al. O-(2-[<sup>18</sup>F]fluoroethyl)-L-tyrosine and L-[methyl-<sup>11</sup>C]methionine uptake in brain tumours: initial results of a comparative study. *Eur J Nucl Med.* 2000;27:542–549.